Electronic properties of potassium-intercalated C_{60} peapods

X. Liu,[1] T. Pichler,[1] M. Knupfer,[1] J. Fink,[1] and H. Kataura[2]
[1]*Leibniz-Institut für Festkörper- und Werkstoffforschung Dresden, D-01069 Dresden, Germany*
[2]*Department of Physics, Tokyo Metropolitan University, 1-1 Minami-Ohsawa, Hachioji, Tokyo 192-0397, Japan*
(Received 16 September 2003; revised manuscript received 23 October 2003; published 27 February 2004)

We present a study of the electronic structure of potassium-intercalated C_{60}-filled single-wall carbon nanotubes (SWCNT's), so-called peapods, in comparison to the corresponding reference SWCNT's. The structural changes and the variation of the electronic properties were characterized by electron energy-loss spectroscopy in transmission. The analysis of the C 1*s* core-level excitations shows that the doping level is nearly the same for peapods and the reference SWCNT's and that a competitive charge transfer of the K 4*s* electrons to both the C_{60} peas and the SWCNT pods occurs. The intercalation process causes an expansion of the intertube distance in the bundle lattices and a decrease of the intermolecular distance between the C_{60} peas in the doped peapods. Regarding the optical properties, the charge transfer to the peapods (SWCNT's) yields the formation of a free-charge-carrier plasmon at about 1.3 eV (1.45 eV). An analysis by an effective Drude-Lorentz model shows that the lower plasmon energy in the doped peapods can be explained by a higher effective screening in these hybrid compounds.

DOI: 10.1103/PhysRevB.69.075417 PACS number(s): 73.61.−r, 78.67.Ch, 78.66.Tr

I. INTRODUCTION

Single-wall carbon nanotubes (SWCNT's) have attracted much attention due to their remarkable properties such as high stiffness, high thermal conductivity, and a tunable electrical conductivity between a semiconducting and a metallic behavior.[1] Moreover, they are also of fundamental interest since they are a very good approximation of a one-dimensional object. Recently, several groups have reported the observation of the encapsulation of fullerenes (e.g., C_{60}) inside SWCNT's, so-called peapods.[2–4] These materials represent a new class of hybrid systems where the fullerenes form one-dimensional molecular chains within nanotubes and the encapsulated C_{60} peas are van der Waals bonded. Within a high-temperature treatment in vacuum, the peapods can act as a template for the creation of double-wall carbon nanotubes.[5] Scanning tunneling spectroscopy experiments on individual peapods[6] have shown that the C_{60} encapsulated in the semiconducting SWCNT affect the local electronic structure of the tube. Especially the local density of states in the conduction band is modulated with the period of the underlying C_{60} array due to a weak coupling between the C_{60} and SWCNT's.[7] The unoccupied electronic density of states as probed by core-level electron energy-loss experiments and the optical properties however are only weakly perturbed in comparison to those of pure C_{60} and pure SWCNT's.[8]

As far as future applications of carbon materials are concerned, the controlled modification of physical properties of these materials by means of intercalation is of considerable interest. For instance, the electrochemical reactivity and the porosity make lithium-intercalated SWCNT's attractive for the usage in Li-ion batteries.[9] In the past, detailed studies of the doping by intercalation have been performed extensively for the intercalation compounds of fullerenes[10] (FIC) and graphite[11] (GIC). For the intercalation of SWCNT's, in contrast to FIC and GIC, no distinct intercalation stages were observed so far. Alkali-metal intercalation of mats of bundled SWCNT's takes place inside the channels of the triangular bundle lattice and leads to a shift of the Fermi energy, a loss of optical transitions,[12] and an increase of the conductivity by about a factor of 30.[13–15] A complete charge transfer between the donors and the SWCNT's was observed up to saturation of doping, which was achieved at a carbon to alkali-metal ratio of about 7,[13,15] which is similar to the highest doping in GIC KC_8 (Refs. 11 and 16) and FIC K_6C_{60}.[17] Furthermore, doped SWCNT's can also be obtained by performing electrochemical redox reactions between SWCNT thin films and solutions of organic radical anions.[18,19] Most of the experimental work regarding the charge transfer and optical properties of intercalated SWCNT's has been done using Raman spectroscopy.[20–23] A stable phase for intermediate doping level for alkali-metal doped SWCNT's has been predicted, which leads to the nonmonotonic changes of the Raman spectra.[21] Regarding the intercalation of peapods, Raman results on potassium intercalation of C_{60} peapods revealed that at high levels in addition to a charge transfer to the SWCNT pods the C_{60} peas are also charged up to $(C_{60})^{6-}$ and form a metallic one-dimensional polymer.[24] At intermediate doping in contrast to the FIC, a continuous charge transfer to the SWCNT's and the C_{60} peas is observed as a function of dopant concentration.[25] This is in contrast to results from electrochemical doping that do not show a charge transfer to the C_{60} peas,[26] which points out that a higher doping level can be achieved with potassium intercalation.

In this contribution, we present a detailed study of the changes of the structural and electronic properties of K-intercalated C_{60} peapods using high-resolution electron energy-loss spectroscopy (EELS) in transmission. The modulation of the bundle structure and the intermolecular distance within peapods due to intercalation is reflected in the variations of the diffraction patterns. The charge transfer from K to peapods significantly affects the intensity of the interband transitions and results in a free-charge-carrier plasmon. We will show that at saturation doping the same K concentration and doping level can be reached for intercalation of both peapods and SWCNT's. The measured loss functions are analyzed within a Drude-Lorentz model for both doped pea-

pods and SWCNT's for comparison. The lower-energy position of the charge-carrier plasmon in the doped peapods can be explained by the partial charge transfer to C_{60} molecules and the remarkable enhancement of the dielectric background with doping.

II. EXPERIMENT

The pristine SWCNT's used for our studies were produced by laser ablation, purified, and filtrated into mats of a buckypaper as described previously.[27,28] The diameter of the SWCNT's is about 1.4 ± 0.1 nm as determined by electron-diffraction and optical absorption spectroscopy.[29] The C_{60} peapods in this experiment were produced in a two-step process. The SWCNT's are purified and opened, and then they are filled by exposure to a fullerene vapor at high temperature.[3] For the EELS measurements, thin films of peapods and reference SWCNT's with an effective thickness of about 100 nm were prepared by dropping an acetone suspension of the materials onto KBr single crystals. After KBr was dissolved in distilled water, the films were transferred to a standard 200 mesh platinum electron microscopy grid and heated to 620 K for several hours in ultrahigh vacuum to remove organic contaminations in the films. Subsequently, the films were transferred into the measurement chamber (base pressure 2×10^{-10} mbar) of a purpose-built 170 keV EELS spectrometer.[30] The energy and momentum resolution was set to 180 meV and 0.03 $Å^{-1}$ for the low-energy-loss function (valence-band excitations) and electron diffraction and to 300 meV and 0.1 $Å^{-1}$ for the core-level excitations, respectively. All measurements are performed at room temperature. Measurements of the filling factor using the bulk sensitive EELS revealed a C_{60} occupancy of about 92% in the present peapods.[8]

The intercalation process was carried out *in situ* in an ultrahigh vacuum chamber by evaporation of K from commercial SAES getter sources. During potassium evaporation, the film was kept at 400 K and further annealed for 20 min at the same temperature to improve intercalant homogeneity and remove any possible excessive K from the film surface. This process was repeated several times until maximum intercalation was reached as revealed by a saturation in all characteristic changes discussed in this paper below.

III. RESULTS AND DISCUSSION

A. Core-level excitations

Information on the electronic structure of intercalated peapods and SWCNT's can be extracted from the analysis of the core-level excitations from the C $1s$ level. The measured core edge structure in EELS spectra corresponds directly to electronic transitions into unoccupied states with C $2p$-related π^* and σ^* character. For the SWCNT's, the former is characterized by a nearly symmetric peak centered at around 285.4 eV, while the latter starts at around 292 eV. Although these peaks give a measure of the carbon derived matrix element weighted density of states, a detailed analysis is complicated by the fact that both are strongly excitonic in nature.[13,15] The same effect also holds for the peapods. In addition, the corresponding response from C_{60} is also present as can be seen, e.g., by the small peak between π^* and σ^* states in the spectrum of the pristine peapods (see Fig. 1).

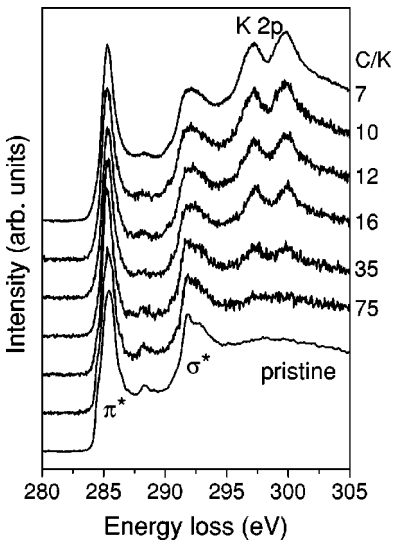

FIG. 1. Core-level excitations of the pristine and doped peapods for different K concentrations as indicated by the C/K ratio.

In the doped compounds, the intercalation level can be monitored by the relative intensity of the C $1s$ to K $2p$ core-excitations.[15] As can be seen in Fig. 1, with increasing K intercalation, at the higher-energy range the signal of the K $2p$ excitations is present. This excitation becomes stronger with increasing K content. In addition, the σ^* related features are washed out upon increasing K addition. The potassium concentration is indicated by the C/K ratio, which can be estimated after normalizing the spectra to the inflection point of the σ^* onset taking a well-known stoichiometry such as GIC KC_8 as reference.[15] A maximal C/K ratio of about 7 is observed for both peapods and SWCNT's. The two excitonic transitions (into π^* and σ^* states) in the pristine peapods and SWCNT's are only weakly influenced by the alkali-metal intercalation. Their line shape and their positions remain unchanged after full doping. Due to the presence of C_{60}, the peapods have a higher amount of carbon atoms and the maximal C/K=7 explicitly shows that the C_{60} peas are most likely also charged in the intercalation process. The maximum C/K ratio in potassium-intercalated K_6C_{60} is 10. Taking into account the filling factor and that there are about 36% more carbon atoms from the peas, we estimate a maximum C/K=7.5, which is slightly higher than the observed value. In addition, one can take into account the doping-induced polymerization of the peas.[24] Assuming that one extra electron is required for the polymer bond, a maximum C/K=7.3 is obtained, which, within experimental error, is the same as for the intercalated SWCNT's. Hence, the saturation of doping is only determined by the charge storage capacity of the intercalated carbon compounds and the C_{60} peas are charged at least up to $(C_{60})^{-6}$.

In order to extract more information about the electronic structure in the conduction band it is interesting to compare the C $1s$ spectra of the pristine and the fully intercalated peapods with those of SWCNT's as depicted in the left panel

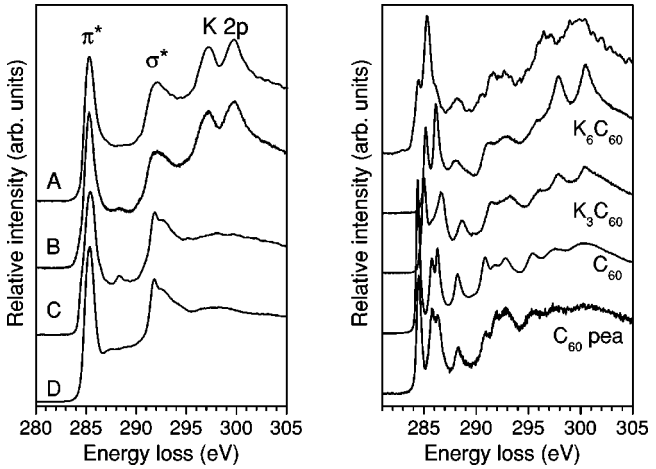

FIG. 2. Left panel: Core-level excitations of the pristine (*C*) and the fully K-intercalated peapods (*B*) compared with the corresponding spectra of the pristine (*D*) and doped (*A*) SWCNT's. Right panel: Core-level excitations of the extracted doped peas (top) in comparison with those of K_6C_{60}, K_3C_{60}, and C_{60} in solid (Ref. 31) and the extracted undoped C_{60} peas.

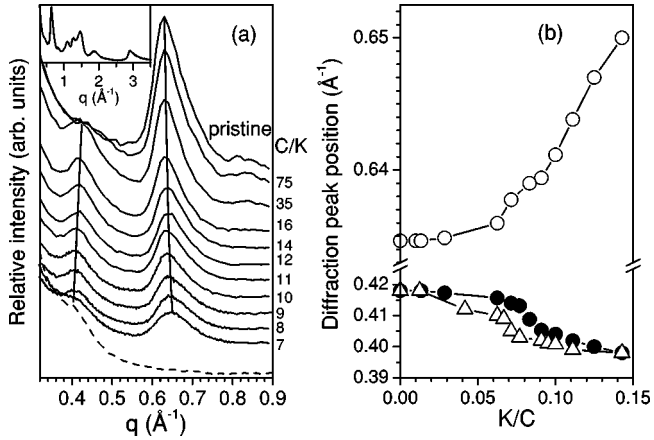

FIG. 3. (a) The evolution of the diffraction pattern of peapods with increasing K concentration as indicated by the corresponding C/K ratio. The almost vertical lines depict the evolution of the first bundle peak at about 0.4 $Å^{-1}$ and of the first C_{60} Bragg reflection at about 0.63 $Å^{-1}$. For comparison, a diffraction pattern of doped SWCNT's with C/K=7 is shown as dashed line. In the inset, the diffraction pattern of pristine peapods is shown in a wider range. (b) The peak position of the first C_{60} peak (○) and of the first bundle peak (●) as a function of the intercalation level. Also shown is the doping dependence of the first bundle peak in potassium-intercalated SWCNT's (△).

of Fig. 2. It can be clearly seen that the spectral shape above the excitation onset is similar for both the peapods and the reference sample except for the small response from C_{60}. Especially, there is no hybridization between peapods and SWCNT π^* states and K valence states, i.e., there is no splitting in the π^* states peak, as compared to GIC KC_8.[32] Though there is a shift of the Fermi level to the conduction band due to K doping, the strong excitonic effect of the π^* resonance renders it invisible in the C 1*s* core-level excitation spectrum. In addition, the amount of charge transfer in the doped SWCNT's can be monitored by the decrease of the π^* resonance spectral weight. In agreement with previous results on intercalated SWCNT's (Ref. 13) we also observe a decrease of about 10% at full intercalation. This corresponds within the experimental error to a full charge transfer of the K 4*s* electrons into the conduction band of the doped compounds.

To further analyze the electronic structure from C 1*s* EELS and clarify the role of the local bonding environment and charge transfer, it is useful to extract the signal of the doped C_{60} peas from that of the peapods. As was mentioned above, from the edge jump in the core-level excitation spectrum and from the C_{60} shape resonances, the filling factor can be estimated on a bulk scale and the C 1*s* spectrum of the C_{60} peas can be extracted, respectively.[8] In the present sample, after normalization at 305 eV the peapod spectrum had to be scaled by about 1.3 before subtracting the SWCNT reference spectrum to obtain the response of the C_{60} peas. This corresponds to the filling factor of about 92% for SWCNT's with a mean diameter 1.4 ± 0.1 nm.[8] The spectrum of the extracted C_{60} peas using the above-mentioned scaling factor for both the pristine and intercalated peapods is depicted in the right panel of Fig. 2. For comparison, reference spectra of C_{60}, K_3C_{60}, and K_6C_{60} are also shown.[31] In the spectrum of the doped C_{60} species, the filling of the lowest unoccupied molecular orbitals (LUMO) with doping results in the disappearance of the corresponding peak. The spectrum of the K 2*p* doublet reveals that the doping level is like in K_6C_{60} rather than in K_3C_{60}. This is also supported by the charge transfer estimated from a decrease of the overall π^* intensity below the σ^* onset which has the same value as in K_6C_{60} and is therefore consistent with a complete occupation of the LUMO of the C_{60} peas. The overall shape of the response is modified compared to K_6C_{60} which is consistent with the observed formation of a one-dimensional charged C_{60} polymer.[24]

B. Electron diffraction

We also carried out a structural analysis using electron diffraction in the EELS spectrometer by setting the energy-loss to zero, which gave results consistent with those of x-ray-diffraction studies.[33,34] In the inset of Fig. 3(a) the electron-diffraction pattern of the pristine C_{60} peapods is shown. Compared with the corresponding spectrum of the empty SWCNT reference sample, the most obvious difference is that additional diffraction peaks appear for the peapods. The most pronounced Bragg peak is at 0.635 $Å^{-1}$, which is derived from the diffraction of the C_{60} in a one-dimensional arrangement within SWCNT's. The corresponding next-nearest-neighbor distance of two encapsulated C_{60} molecules is about 0.99 nm. In addition, the diffraction of the first bundle peak at around 0.42 $Å^{-1}$ is remarkably suppressed as compared with the SWCNT's due to the change of the scattering factor in the peapods derived from the encapsulation of C_{60}.[33] This behavior is also an evidence of C_{60} molecule encapsulation inside nanotubes.

When the C_{60} peapods are exposed to K vapor, the effect of intercalation is also reflected in changes of the diffraction pattern. Here we focus on the lower *q* region in the range

between 0.3 and 0.9 $Å^{-1}$ where the diffraction peaks from both peas and pods are very pronounced. Figure 3(a) shows the electron-diffraction data of the pristine and K-intercalated peapods samples as a function of the potassium content. It is clearly seen that with increasing potassium concentration, the diffraction peak corresponding to the distance between the encapsulated C_{60} molecules shifts to higher q and its intensity decreases. In addition, the peaks of the SWCNT bundle lattice shifts to lower q. For comparison, the diffraction of the fully doped SWCNT's is also shown as dashed line in the figure. It is obvious that there are no diffraction features in the region around $q=0.65$ $Å^{-1}$ for the doped SWCNT's, which confirms that the diffraction feature in the range of 0.6 and 0.7 $Å^{-1}$ is only from the C_{60} peas. We now turn our attention to a more detailed analysis of the doping dependence of these characteristic diffraction peaks (see Fig. 3). The upshift of the peak corresponding to the separation between the C_{60} peas stands for a decrease of their intermolecular distance from 0.99 to 0.96 nm. In pressure polymerized C_{60} the intermolecular distance is about 0.92 nm.[35] In this case the polymerization is established via a $2+2$ cycloaddition process. In single-bonded polymers the polymer bonds are weaker, which is consistent with the bigger C_{60} separation and supports previous reports of a doping-induced single-bonded polymerization of C_{60} molecules inside SWCNT's.[24] However, as can be seen in Fig. 3(b), the upshift of the peak corresponding to the intermolecular C_{60} separation is monotonous and there is no spontaneous polymerization observed. Further work on oriented samples will allow more insight into the details of this reaction within the peapods. Regarding the amount of expansion of the SWCNT lattice upon intercalation it is useful to compare the electron diffraction of the first bundle peak from the reference SWCNT's and peapods films [Fig. 3(b)]. The results indicate that the lattice expansion in peapods is very similar to that in the reference sample and finally yields the same value of about 1.82 nm at full doping. The decrease in the intensity of this first bundle peak with intercalation mostly results from the insertion of intercalants into the bundle which cause more disorder and thus a decrease of the respective Bragg peak intensity.

C. Optical response

We now focus on the doping dependence of the optical response of peapods following the intercalation with potassium. For each K donor the outer $4s$ electron will be transferred to the peapods. The transferred charge will fill states of the conduction band of peapods and result in a Fermi-level shift to higher energies. This is revealed in the measurements of the low-energy loss function at low momentum transfer. Figure 4 shows the evolution of the loss function of peapods with different K contents starting from the pristine peapods (bottom) in an energy range between 0.2 and 13 eV at $q=0.15$ $Å^{-1}$. In the inset of Fig. 4, the loss function of peapods is shown in a wide range up to 45 eV. One wide peak at around 6 eV is the π plasmon related to a collective excitation of all π electrons of the peapods; the other wide peak at about 23 eV is related to all π and σ electrons and

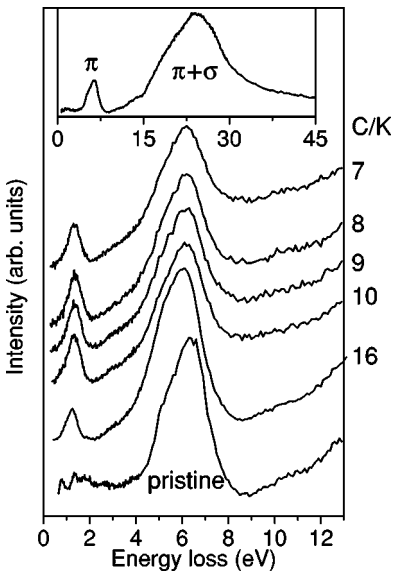

FIG. 4. The low-energy-loss spectra of the pristine and intercalated peapods for different doping levels at $q=0.15$ $Å^{-1}$ in the energy range between 0 and 13 eV after removing the quasielastic scattering background. The inset shows the loss function of the pristine peapods in a wider range covering π and $\pi+\sigma$ plasmons.

hence labeled as $\pi+\sigma$ plasmon. The three loss function peaks in the pristine peapods below 3.0 eV stem from the optically allowed interband transitions from the nanotubes. Due to charge transfer of K $4s$ electrons, the conduction bands are populated with electrons. Consequently, some previously allowed optical transitions are suppressed as their final states become occupied. The evolution of the loss function shows that the interband transitions disappear with increasing potassium concentration and an additional peak occurs in the loss function in the energy range between 1 and 2 eV. Its energy position shifts to higher values with increasing doping levels. Therefore, an origin of this peak due to interband transitions can be ruled out because its energy position then would be roughly independent of intercalation. In keeping with previous results on intercalated SWCNT's the new feature can be safely associated with the collective excitation of the introduced conduction electrons, the so-called charge-carrier plasmon.[13,15]

As can be seen in Fig. 4, the energy position of the charge-carrier plasmon shifts to higher energy values with increasing intercalation levels up to about 1.3 eV. To further analyze the optical properties we have subtracted the quasielastic background as described previously.[15] Figure 5 shows a comparison of the loss functions of different intercalation compounds at saturation of the intercalation in the energy range between 0 and 40 eV at $q=0.15$ $Å^{-1}$. For comparison, the spectra of the SWCNT's C/K=7, GIC KC_8, and peapods C/K=7 are normalized to the $\sigma+\pi$ spectral weight. It can be clearly seen that the charge-carrier plasmon energy of the doped peapods is the lowest one among the three fully doped compounds. Additionally, the intensity of the charge-carrier plasmon is lowest and its width (damping) is highest for the intercalated peapods. The prominent feature at around 6 eV which is assigned to the plasmon oscillation of all π electrons becomes broader with doping as compared with the

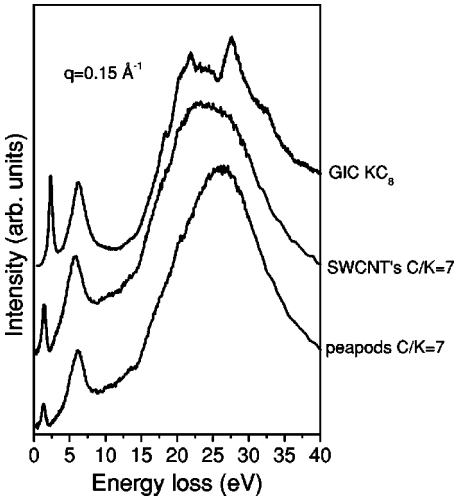

FIG. 5. The low-energy-loss spectra of the fully K-intercalated peapods compared with the fully doped SWCNT's and GIC KC_8 at $q=0.15$ Å^{-1} after background subtraction.

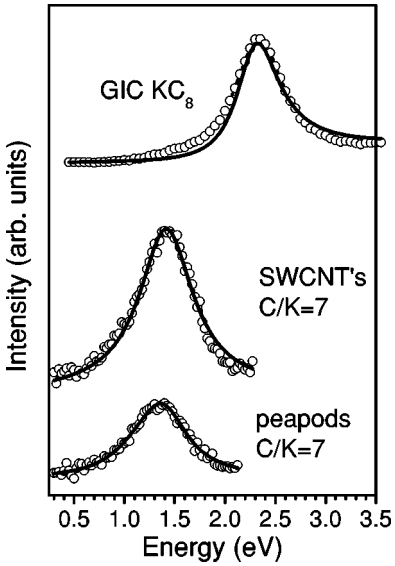

FIG. 6. Analysis of the loss function at $q=0.15$ Å^{-1} in the range of the charge-carrier plasmon for the fully K-intercalated peapods, SWCNT's, and GIC KC_8. The solid lines are results from a Drude-Lorentz model as described in the text. The parameters are listed in Table I.

pristine material. The energy position of the π plasmon in the fully doped peapods is higher than in SWCNT's, but it is lower than in GIC KC_8. Compared with the pristine material, the doping only results in a very slight down-shift of the π plasmon energy for both peapods and SWCNT's. This is in contrast to GIC KC_8 where a pronounced down-shift of the π plasmon from about 7 to 6.3 eV is observed.[32,37] In other words, generally, the electronic levels of peapods and SWCNT's are weakly affected by the intercalation process. Regarding the σ valence electrons, the $\sigma+\pi$ plasmon of the doped peapods has a higher value (the same happens in the pristine material). This is the first hint for a stronger screening of the charge carrier and the π plasmon in the intercalated peapods.

In order to obtain more detailed information about the dielectric properties, the measured loss function was analyzed within the framework of a Drude-Lorentz model, which was successfully applied to describe, e.g., graphite, GIC, FIC, and SWCNT intercalation compounds.[13] In the case of intercalated SWCNT's and GIC, a charge-carrier plasmon, one interband oscillator giving rise to the π plasmon, and another oscillator for the $\pi+\sigma$ plasmon were sufficient to explain the optical properties of the fully doped compounds. As described in detail previously,[13] the impact of the higher-energy plasmon to the lower one can be described by an effective screening with a background dielectric function ϵ_∞ in the doped compounds. The π and $\pi+\sigma$ plasmons screen the charge-carrier plasmon which leads to a shift to lower energies as compared to its unscreened value.

In the fully K-doped SWCNT's, the charge-carrier plasmon peak is fitted with the dielectric background and Drude plasmon. However, for the doped peapods, the contribution from doped peas was also considered. Since we observed a fully occupied LUMO for our doped C_{60} peas we have included one additional transition from K_6C_{60}, which has a fully occupied LUMO in our Drude-Lorentz model. The relative intensity and width of the lowest transition of K_6C_{60} at 1.2 eV were taken from previous experiments[38] considering the scaling factor in the peapods. All other C_{60} related transitions contribute to the dielectric background. The results are depicted in Fig. 6 and the parameters are shown in Table I. It can be clearly seen that the unscreened plasmon energy is almost the same in both fully doped peapods and SWCNT's. But the total dielectric background changes remarkably. It turns out that the dielectric background reached about 6.7 and 8.4 for the fully K-doped SWCNT's and peapods, respectively. Hence, the lower energy of the charge-carrier plasmon in the doped peapods can be attributed to the stronger screening effect due to high background from the doping and the encaged C_{60}.

Furthermore, from the Drude-Lorentz model analysis of the intercalated peapods and SWCNT's, additional information about the optical conductivity can be extracted. Experimental and theoretical studies have shown that intercalation increases the conductivity of SWCNT mats significantly.[14,15] From the parameters in Table I, the real part of the optical conductivity can be calculated for the fully K-doped peapods as compared to doped SWCNT's and GIC KC_8. Within the

TABLE I. Parameters for the charge-carrier plasmons in eV from the simulation of the measured loss function of the fully K-intercalated peapods, SWCNT's, and GIC KC_8. For the peapods an additional oscillator was added to account for the doping of the C_{60} peas. E_p, plasmon energy; Γ, width; E_T, oscillator energy; and ϵ_∞ is the background dielectric function from π and σ electrons.

	Charge carrier				Interband		
	E_p	Γ	ϵ_∞	σ_0 (S/cm)	E_p	E_T	Γ
GIC KC_8	5.8	0.2	6.7	22569			
SWCNT's C/K=7	4.04	0.64	6.7	3429			
peapods C/K=7	4.03	0.51	8.4	4282	1.0	1.2	0.9

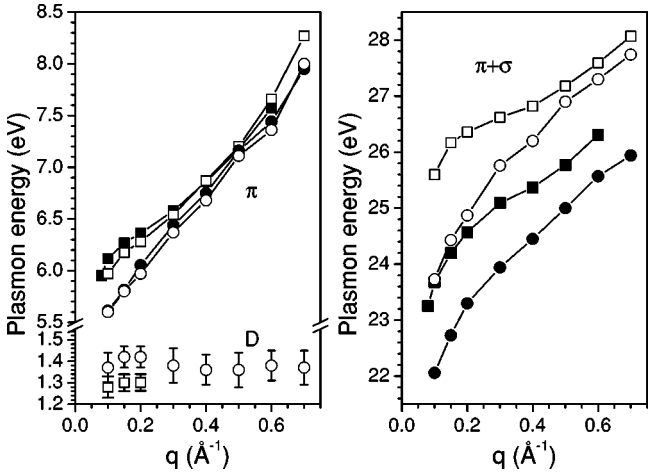

FIG. 7. Left panel: The charge carrier (D) and π plasmon dispersion of the fully doped peapods (□) and SWCNT's (○) compared with the pristine ones (■ and ●). Right panel: The $\pi+\sigma$ plasmon dispersion of the fully doped peapods (□) and SWCNT's (○) compared with the pristine ones (■ and ●).

accuracy of this analysis the extracted dc conductivity of about 4282 S/cm in the fully intercalated peapods is very close to that of doped SWCNT's (3429 S/cm). This is in good agreement with previous measurements of the resistance of an intercalated buckypaper.[24] The calculated values can be directly compared with the results from optical measurement. It can be seen that the Drude-related optical conductivity of the doped peapods is very similar to that of doped SWCNT's but it is much different from the GIC KC_8 (22 569 S/cm). One reason is that the K doping causes the same structural disorder within the nanotube bundles for both peapods and SWCNT's, which is consistent with the above-mentioned electron-diffraction results.

Finally, we turn to the dispersion of the plasmons in the fully doped compounds. The results are shown in Fig. 7. In combination with the well-known one dimensionality of nanotubes the nondispersive peaks in the loss function can be attributed to excitations between localized states which are polarized perpendicular to the nanotube axis and thus resemble molecular interband transitions such as those of C_{60}. In contrast, the π plasmon (at 5.2 eV for low momentum transfer) represents a plasma oscillation of delocalized states polarized along the nanotube axis.[36] As can be seen in Fig. 7, the plasmon dispersion relations are rather similar for fully doped peapods and intercalated SWCNT's. The π plasmon disperses linearly to higher energies with increasing momentum and the dispersion is very similar to that found for the π plasmon in the pristine peapods. However, the plasmon energy is slightly lower than that of the pristine one. This again indicates that the electronic states of nanotubes are to a large extent only slightly affected by the intercalation process.

In contrast to the π plasmon, the charge-carrier plasmon of the doped peapods does not show a dispersion, or only a very weak dispersion. It is also very similar to that of the doped SWCNT's.[13] Since the plasmon dispersion is proportional to the mean Fermi velocity, this indicates that the Fermi velocity of doped peapods and SWCNT's is rather small, a conclusion which is consistent with the arguments above that in fully intercalated compounds the Fermi level lies in a flat band region. Furthermore, with increasing momentum transfer the intensity of the charge-carrier plasmon decreases very rapidly and almost disappears above 0.3 Å^{-1} which renders it difficult to follow its energy position at higher momentum. The drastic decrease in intensity can be ascribed to a damping of the plasmon as a result of a decay into interband excitations between valence and conduction bands in intercalated compounds (Landau damping).[32]

For the $\pi+\sigma$ plasmon, the dispersion is shown in the right panel in Fig. 7. In the pristine material, the C_{60} encapsulated in the SWCNT's increases the total electron density of the valence band and the plasmon energy of peapods is higher than that of SWCNT's. Their dispersion is also positive, i.e., the $\pi+\sigma$ plasmon upshifts with increasing momentum transfer. In the case of the doped compounds, the energy position of the $\pi+\sigma$ plasmon is higher than that of the pristine material. This can be assigned to the contribution of the potassium electrons. The $\pi+\sigma$ plasmon monotonously increases in energy as a function of momentum transfer. The gradient of the doped peapods is somewhat lower than that of the doped SWCNT's.

IV. SUMMARY

We presented a study of the electronic structure of K-intercalated C_{60} peapods in comparison to the corresponding reference compounds from SWCNT's. The structural changes and the variation of the electronic properties were characterized by EELS in transmission. The intercalation causes an expansion of the intertube distance in the bundle lattices and shrinks the intermolecular distance of the C_{60}-C_{60} chain in the peapods. The lattice expansion of the bundle is nearly the same in both the fully doped peapods and SWCNT's. The analysis of the C 1*s* and K 2*p* core-level excitations shows that the doping level is the same for peapods and the reference SWCNT's within the experimental error. The electrons transferred from K to peapods and SWCNT's can fill the lower-energy conduction bands and give rise to the appearance of a charge-carrier plasmon in the intercalated compounds. The energy position of charge-carrier plasmon in the doped peapods is always lower than that of SWCNT's which can be attributed to the increase of the dielectric background in the K-doped peapods as compared with the doped SWCNT's. The unscreened plasmon is nearly the same in the two cases. Hence, the behavior upon intercalation is similar in the peapods and the empty SWCNT's, and the maximum doping level is only determined by the charge storage capacity of the analyzed carbon compounds.

ACKNOWLEDGMENTS

We acknowledge financial support from Grant No. DFG PI440. H.K. thanks the Grant-in-Aid for Scientific Research (A) Grant No. 13304026 from the Ministry of Education, Culture, Sports, Science and Technology of Japan.

[1] R. Saito, G. Dresselhaus, and M.S. Dresselhaus, *Physical Properties of Carbon Nanotubes* (Imperial College Press, London, 1998).
[2] B.W. Smith, M. Monthioux, and D.E. Luzzi, Nature (London) **396**, 323 (1998).
[3] H. Kataura, T. Kodama, K. Kikuchi, K. Hirahara, K. Suenaga, S. Iijima, S. Suzuki, W. Krätschmer, and Y. Achiba, in *Nanonetwork Materials: Fullerenes, Nanotubes, and Related Systems* edited by Susumu Saito, Tsuneya Ando, Yoshihiro Iwasa, Koichi Kikuchi, Mototoda Kobayashi, and Yohachi Saito, AIP Conf. Proc. 590 (AIP, Melville, NY, 2001), p. 165.
[4] K. Hirahara, Y. Maniwa, K. Suenaga, S. Bandow, H. Kato, T. Okazaki, H. Shinohara, and S. Iijima, Phys. Rev. Lett. **85**, 5384 (2000).
[5] S. Bandow, F. Kokai, K. Takahashi, M. Yudasaka, L.C. Qin, and S. Iijima, Chem. Phys. Lett. **337**, 48 (2001).
[6] D.J. Hornbaker, S.J. Khang, S. Misra, B.W. Smith, A.T. Johnson, E.J. Mele, D.E. Luzzi, and A. Yazdany, Science **295**, 828 (2002).
[7] Y. Cho, S. Han, G. Kim, H. Lee, and J. Ihm, Phys. Rev. Lett. **90**, 106402 (2003).
[8] X. Liu, T. Pichler, M. Knupfer, M.S. Golden, J. Fink, H. Kataura, Y. Achiba, K. Hirahara, and S. Iijima, Phys. Rev. B **65**, 045419 (2002); X. Liu, T. Pichler, M. Knupfer, J. Fink, and H. Kataura, Synth. Met. **135–136**, 715 (2003).
[9] H. Shimoda, B. Gao, X.P. Tang, A. Kleinhammes, L. Fleming, Y. Wu, and O. Zhou, Phys. Rev. Lett. **88**, 015502 (2002).
[10] See, e.g., M.S. Dresselhaus, G. Dresselhaus, and P.C. Eklund, *Science of Fullerenes and Carbon Nanotubes* (Academic Press, San Diego, 1996).
[11] M.S. Dresselhaus and G. Dresselhaus, Adv. Phys. **30**, 139 (1981).
[12] R. Jacquemin, S. Kazaoui, D. Yu, A. Hassanien, N. Minami, H. Kataura, and Y. Achiba, Synth. Met. **115**, 283 (2000); S. Kazaoui, N. Minami, R. Jacquimin, H. Kataura, and Y. Achiba, Phys. Rev. B **60**, 13 339 (1999).
[13] X. Liu, T. Pichler, M. Knupfer, and J. Fink, Phys. Rev. B **67**, 125403 (2003).
[14] R.S. Lee, H.J. Kim, J.E. Fischer, A. Thess, and R.E. Smalley, Nature (London) **338**, 255 (1997).
[15] T. Pichler, M. Sing, M. Knupfer, M.S. Golden, and J. Fink, Solid State Commun. **109**, 721 (1999).
[16] J.E. Fischer, J.M. Bloch, C.C. Shieh, M.E. Preil, and K. Jelley, Phys. Rev. B **31**, 4773 (1985).
[17] O. Zhou, J.E. Fischer, N. Coustel, S. Kycia, and Q. Zhu, Nature (London) **351**, 462 (1991).
[18] P. Petit, C. Mathis, C. Journet, and P. Bernier, Chem. Phys. Lett. **305**, 370 (1999).
[19] L. Kavan, P. Rapta, and L. Dunsch, Chem. Phys. Lett. **328**, 363 (2000); A. Claye, J.E. Fischer, and A. Metrot, *ibid.* **333**, 16 (2001).
[20] A.M. Rao, E. Richter, S. Bandow, B. Chase, P.C. Eklund, K.A. Williams, S. Fang, K.R. Subbaswamy, M. Menon, A. Thess, R.E. Smalley, G. Dresselhaus, and M.S. Dresselhaus, Science **275**, 187 (1997).
[21] N. Bendiab, E. Anglaret, J.-L. Bantignies, A. Zahab, J.L. Sauvajol, P. Petit, C. Mathis, and S. Lefrant, Phys. Rev. B **64**, 245424 (2001).
[22] Y. Iwasa, H. Fudo, Y. Yatsu, T. Mitani, H. Kataura, and Y. Achiba, Synth. Met. **121**, 1203 (2001).
[23] A. Kukovecz, T. Pichler, R. Pfeiffer, and H. Kuzmany, Chem. Commun. (Cambridge) **12**, 1730 (2002); A. Kukovecz, T. Pichler, R. Pfeiffer, C. Kramberger, and H. Kuzmany, Phys. Chem. Chem. Phys. **5**, 582 (2003).
[24] T. Pichler, H. Kuzmany, H. Kataura, and Y. Achiba, Phys. Rev. Lett. **87**, 267401 (2001).
[25] T. Pichler, A. Kukovecz, H. Kuzmany, H. Kataura, and Y. Achiba, Phys. Rev. B **67**, 125416 (2003).
[26] L. Kavan, L. Dunsch, and H. Kataura, Chem. Phys. Lett. **361**, 79 (2002).
[27] O. Jost, A.A. Gorbunov, W. Pompe, T. Pichler, R. Friedlein, M. Knupfer, M. Reibold, H.-D. Bauer, L. Dunsch, M.S. Golden, and J. Fink, Appl. Phys. Lett. **75**, 2217 (1999).
[28] H. Kataura, Y. Kumazawa, Y. Maniwa, I. Umezu, S. Suzuki, Y. Ohtsuka, and Y. Achiba, Synth. Met. **103**, 2555 (1999).
[29] X. Liu, T. Pichler, M. Knupfer, M.S. Golden, J. Fink, H. Kataura, and Y. Achiba, Phys. Rev. B **66**, 045411 (2002).
[30] J. Fink, Adv. Electron. Electron Phys. **75**, 121 (1989).
[31] M. Knupfer, Surf. Sci. Rep. **41**, 1 (2001).
[32] L.A. Grunes and J.J. Ritsko, Phys. Rev. B **28**, 3439 (1983).
[33] M. Abe, H. Kataura, H. Kira, T. Kodama, S. Suzuki, Y. Achiba, K. Kato, M. Takata, A. Fujiwara, K. Matsuda, and Y. Maniwa, Phys. Rev. B **68**, 041405 (2003).
[34] A. Thess, R. Lee, P. Nikolaev, H. Dai, P. Petit, J. Robert, C.H. Xu, Y.H. Lee, S.G. Kim, A.G. Rinzler, D.T. Colbert, G.E. Scuseria, D. Tomanek, J.E. Fischer, and R.E. Smalley, Science **273**, 483 (1996).
[35] Y. Li, J. Rhee, D. Singh, and S. Sharma, Phys. Rev. B **68**, 024106 (2003).
[36] T. Pichler, M. Knupfer, M.S. Golden, J. Fink, A.G. Rinzler, and R.E. Smalley, Phys. Rev. Lett. **80**, 4729 (1998).
[37] J.J. Ritsko, Phys. Rev. B **25**, 6452 (1982); D.M. Hwang, M. Ultraut, and S.A. Solin, Synth. Met. **3**, 81 (1981).
[38] T. Pichler, M. Matus, J. Kürti, and H. Kuzmany, Solid State Commun. **81**, 859 (1992).